JOURNAL OF MECHANICAL ENGINEERING AND SCIENCES (JMES)
ISSN: 2289-4659 e-ISSN: 2231-8380
VOL. 15, ISSUE 1, 7695 – 7714
DOI: https://doi.org/10.15282/jmes.15.1.2021.07.0607

ORIGINAL ARTICLE

Energy harvesting from car suspension system: Mathematical approach for half car model

T. Darabseh[1], D. Al-Yafeai[1] and A-H.I. Mourad[1,2]

[1] Department of Mechanical Engineering, College of Engineering, United Arab Emirates University, Al-Ain, P.O. Box. 15551, United Arab Emirates
Phone: +6094246234; Fax: +609424222
[2] Mechanical Design Department, Faculty of Engineering, El Mataria, Helwan University, Cairo, P.O. Box. 11718, Egypt

ABSTRACT – A significant contribution of this paper is developing a half car model with a built-in piezoelectric stack to evaluate the potential of harvesting power from the car suspension system. The regenerative car suspension system is modelled mathematically using Laplace transformation and simulated using MATLAB/Simulink. Two piezoelectric stacks are installed in series with the front and rear suspension springs to maintain the performance of the original suspension system in ride quality and comfortability. Half car model is subjected under harmonic excitation with acceleration of 0.5 g and velocity of 9.17 rad/s. The harvested voltage and power are tested in both time, and frequency domain approaches. The influence of the different parameters of the piezoelectric stack (number of stack layers and area to thickness) and car suspension (sprung and unsprung stiffness and damping coefficients) are examined. Also, the effect of road amplitude unevenness is considered. The results illustrate that the maximum generated voltage and power at the excitation frequency of 1.46 Hz are 33.51 V and 56.25 mW, respectively.

ARTICLE HISTORY
Received: 17th Dec 2019
Revised: 15th May 2020
Accepted: 21st Aug 2020

KEYWORDS
Energy harvesting;
piezoelectric stack method;
car suspension;
half car model;
analytical modelling

INTRODUCTION

Recent researches are focused on harvesting the loss of vibration energy into useful electrical energy. Dampers of the car suspension system are the main source of the vibration losses. [1, 2]. There are several mechanisms discussed in harvesting car's mechanical vibrations such as, attaching multiple piezoelectric harvesters [3–14], electromagnetic [15–19], electrostatic transducers [20], linear electromagnetic shock absorber, MR electromagnetic regenerative damper, hydraulic, rack-pinion, ball-screw, and cable/pullies [21–26]. However, Piezoelectric harvester is one of the most efficient and desirable transducer because of its simplicity, operate in the wide frequency range, excellent electromechanical coupling, and producing the highest power density [27–30]. The work in installing the piezoelectric energy transducer in a car suspension system has been discussed by some researchers; however, more attention should be paid to this issue. Most of the studies were focused on evaluating the dissipated energy from the car suspension system not the harvested energy [21]. Wei and Taghavifar [31] evaluated the power dissipation from a half car model. The dissipated power by the front suspension was greater than the rear car suspension by 35%. The reason behind this variation is the high values of the front suspension parameters compared with the rear parameters.

For energy harvesting applications, two primary groups of piezoelectric materials are divided into two main groups including in piezo-ceramics such as Lead Zirconate Titanate (PZT) or Barium Titanate (BaTiO3), and piezo-polymers like Polyvinylidene Fluoride (PVDF). Many energy harvesting works are oriented to utilizing the Lead Zirconate Titanate (PZT) type due to its advantages. The PZT film coefficient is at least two times greater than the other types which helps in providing high power output [32]. As reported by Makki and Iliev, PZT has harvested power output per unit area of 9.37×10^{-3}mW/mm^2 while, PVDF has harvested a lower value of 5.31×10-4mW/mm^2 [33].

Piezoelectric materials could be attached in different locations in car suspension system. Attaching piezoelectric harvesters to the car springs is one of the possible ways as they will generate electrical charge across their terminals when the vehicle is subjected to the road vibrations and cause the springs to strain [3, 13]. Namuduri et al. [3] developed an energy harvesting system by attaching a layer of piezoelectric composite fiber on top of the four surfaces of the leaf springs. The harvesting system generates electricity due to the compressions and tensions of the spring during the car travel. Each piezoelectric element is coupled to a rectifier to convert the AC output voltage to DC that is used in powering multiple devices in the vehicle or storing it in a battery or capacitor. They reported that the generated electric charge is proportional to the level of stress σ or strain S applied to the springs, more deformation subjected to the harvester will generate more electrical charge . Wang et al. [4] modelled the harvesting system as a quarter car model with attaching a piezoelectric element in parallel with the spring of the suspension system. The system was able to generate a theoretical power up to 2.84W when subjected to a sine wave acceleration of 1g. The efficiency of the energy harvesting system was affected by the tire stiffness, suspension spring stiffness, and a suspension damping coefficient. The theoretical analysis results such as resonant frequencies, harvested voltage, and the effect of the various external resistances were validated experimentally by modeling the car body and tires as aluminum blocks. However, Al-Yafeai et al. [5] compared the

*CORRESPONDING AUTHOR | A-H.I. Mourad | ✉ ahmourad@uaeu.ac.ae

results of the harvested energy from Wang's quarter model [4] with their proposed half car model by inserting two piezoelectric materials in the front and rear suspension system. The findings show that, there was an increase in the harvested voltage and power by about 77% and 57%, respectively. The output voltage and power from Wang et al. [4] and Doaa et al. [5] models were calculated without considering the stiffness coefficient of the piezoelectric element which will profoundly affect the magnitude of both harvested voltage and power. Considering the value of the piezoelectric stiffness coefficient and installing it in parallel with the suspension system will increase the overall stiffness of the system and this significantly decreases the harvested voltage and power from W to mW due to the less deformation of the piezoelectric material.

Piezoelectric energy harvester can also be mounted on the vehicle wheels as it will produce electricity due to the deformation of the wheels. Xie and Wang [6] built a dual mass piezoelectric bar harvester placed on the wheels of the car suspension system. They have modeled it as a spring and a damper in the mathematical model. A piezoelectric material was made of PZT-4 (lead zirconate titanate) with a width of 1.5 cm and a height of 10 cm without specifying the number of layers. The model was subjected to different classes of road roughness classified by ISO/TC108/SC2N67 starting from a very smooth to a poor road surface. From a road profile of class D, which means inferior road surface, the system has a potential power of 738 W that could be attained by inserting more than four piezoelectric harvesters to the system. They have mentioned that, the resultant power is influenced by several factors such as the input car velocity, road roughness irregularity, and the dimensions of the piezoelectric element.

Piezoelectric materials can be mounted in the inner circumference of the tires and connected to the capacitor for storing the electrical charge. Behera [7] connected 32 piezoelectric modules of type PZT-5A that were arranged in three strips connected in series. The model was able to harvest the power of 14 mW per wheel rotation per second at velocity travel of 40km/h. Whereas, Lafarge et al. [8] assembled a cantilever piezoelectric beam of type PZT-27 into the wheels of the car. The quarter car model was excited at 91Hz that relates to the first natural frequency of the cantilever beam. The harvested power was evaluated with two different loads resistance: 22kΩ and 222kΩ. The peak values were reported as 1 mW and 1.4 mW, respectively, which can be powered several sensors for monitoring applications. The system was also investigated in real case by installing the piezoelectric beam into the unsprung mass. At speed car of 10km/h, the harvested power was varied between 0.001 mw and 0.021 mW. However, the harvested power of the range of 0.01mW and 0.07mW was occurred at 30 km/h.

Additionally, piezoelectric material could be designed as a regenerative shock absorber that will generate electricity from the variation of fluid pressure due to piston displacement in the dampers. The piston compresses the fluid inside the damper and creates pressure when it is exposed to vibration. The resulting fluid pressure causes the deformation of the piezoelectric plates and consequently produces an electric charge. Lee et al. [9] installed two parallel plates of piezoelectric material of type PZT-4 in the suspension shock absorber. At the excitation frequency of 10Hz, the output voltage and power generated were about 20V and 1.2mW, respectively. However, Lafarge et al. [10] studied the effect of the location of piezoelectric material in the shock absorber, whether to be stacked on the damper's surface (d31) or placed between two surfaces (d33). At speed of 30km/h, the results showed that PZT-5H harvested a higher power (6mW) when it is in the mode d33, while, the power of 3 mW was recorded in the mode d31.

Another approach to increase the harvested energy from car suspension system is using a multilayer piezoelectric stack [11–14]. Arizti [13] implemented a PZT stack on the top part of the piston in the shock absorber. Due to the significant disturbance in front wheel compare it to the rear one, the system was able to generate a voltage of 17.69mV from the front wheel per one bump in the road. The harvested power from their proposed system was not mentioned. They have reported that, increasing the effectiveness of a multilayer PZT stack depends on increasing the thickness of the piezoelectric layers or increasing the number of layers. Hendrowati et al. [14] built a system with multilayer piezoelectric mechanism to increase the performance of the piezoelectric harvester. This mechanism was able to convert the relative vertical displacement into horizontal displacement in order to reduce the relative displacement and amplify the spring force. The PZT stack mechanism was connected in series with the suspension's spring, and this led to generate a power of 7.17 times larger than the direct mounting to the car suspension system. The harvesting energy from the suspension system can be also used to control the vibrations in the system by implementing a piezoelectric stack in the shock absorber. Ali and Adhhikari [11] established a dynamic vibration absorber that is modeled as two degrees of freedom (2 DOF) system coupled with the electric circuit. The harvesting system was subjected to the sinusoidal excitation at a constant frequency, while Madhav and Ali [12] excited the same system with random input excitation. The aim of the two researches was to find the optimal mechanical and electrical parameters in order to get the maximum power output and minimum system's vibrations.

It can be concluded from the previous studies that most of the work was performed considering quarter car model (2 DOF) which does not imitate the real functions of the car. Furthermore, energy harvesting researches on the suspension system were oriented to modify the shock absorbers in the system that will affect the performance of the suspension system from different aspects in road handling, and ride quality. The current work aims to develop a half car model with attaching two piezoelectric stacks in series with the suspension's springs. This technique will not cause any change in the performance of the car suspension system. The piezoelectric parameters, as well as the suspension parameters, are investigated. Piezoelectric energy harvesting system is built and modelled using a MATLAB/Simulink.

MATHEMATICAL MODEL

Mechanical System without Piezoelectric Stack

Different mathematical models are used for analyzing the vehicle dynamics. Quarter-car model is one of the simplest and mostly used in the car suspension analysis. It represents one-quarter of the car body connected to one tire, where each of them has only the bouncing motion. However, half car model analyzes the half car body connected to front and rear tires. It examines both the bouncing and pitching modes of vibrations. In this work, four degrees of freedom model is built and illustrated in Figure 1. The equations of motion are developed applying Newton's 2nd law as follows:

The equation of the bouncing motion of the front unsprung mass:

$$M_{uf}\ddot{Y}_{uf} = -K_{uf}\left(Y_{uf} - Y_{Rf}\right) - b_{uf}\left(\dot{Y}_{uf} - \dot{Y}_{Rf}\right) + K_{sf}\left(Y_s - L_f\theta_s - Y_{uf}\right) + b_{sf}\left(\dot{Y}_s - L_f\dot{\theta}_s - \dot{Y}_{uf}\right) \quad (1)$$

The equation of the bouncing motion of the rear unsprung mass:

$$M_{ur}\ddot{Y}_{ur} = -K_{ur}(Y_{ur} - Y_{Rr}) - b_{ur}\left(\dot{Y}_{ur} - \dot{Y}_{Rr}\right) + K_{sr}(Y_s + L_r\theta_s - Y_{ur}) + b_{sr}\left(\dot{Y}_s + L_r\dot{\theta}_s - \dot{Y}_{ur}\right) \quad (2)$$

The equation of the bouncing motion of the sprung mass:

$$M_s\ddot{Y}_s = -K_{sf}\left(Y_s - L_f\theta_s - Y_{uf}\right) - b_{sf}\left(\dot{Y}_s - L_f\dot{\theta}_s - \dot{Y}_{uf}\right) - K_{sr}(Y_s + L_r\theta_s - Y_{ur}) - b_{sr}\left(\dot{Y}_s + L_r\dot{\theta}_s - \dot{Y}_{ur}\right) \quad (3)$$

The equation of the pitching motion of the sprung mass:

$$I_s\ddot{\theta}_s = L_f[K_{sf}\left(Y_s - L_f\theta_s - Y_{uf}\right) + b_{sf}\left(\dot{Y}_s - L_f\dot{\theta}_s - \dot{Y}_{uf}\right)] - L_r\left[K_{sr}(Y_s + L_r\theta_s - Y_{ur}) + b_{sr}\left(\dot{Y}_s + L_r\dot{\theta}_s - \dot{Y}_{ur}\right)\right] \quad (4)$$

The road profile is modelled as a harmonic acceleration excitation that excites the vehicle front tire $\ddot{Y}_{Rf}$ (t) and the rear tire with the following delayed function $\ddot{Y}_{Rr}$ (t):

$$\ddot{Y}_{Rr}(\tau) = \ddot{Y}_{Rf}(\tau - T) \qquad \text{where} \qquad \ddot{Y}_{Rf}(\tau) = \text{asin}(\omega\tau) \quad (5)$$

where a is the acceleration amplitude of the sine wave, ω is the angular frequency, and T is the time delay that depends on the vehicle wheelbase and velocity

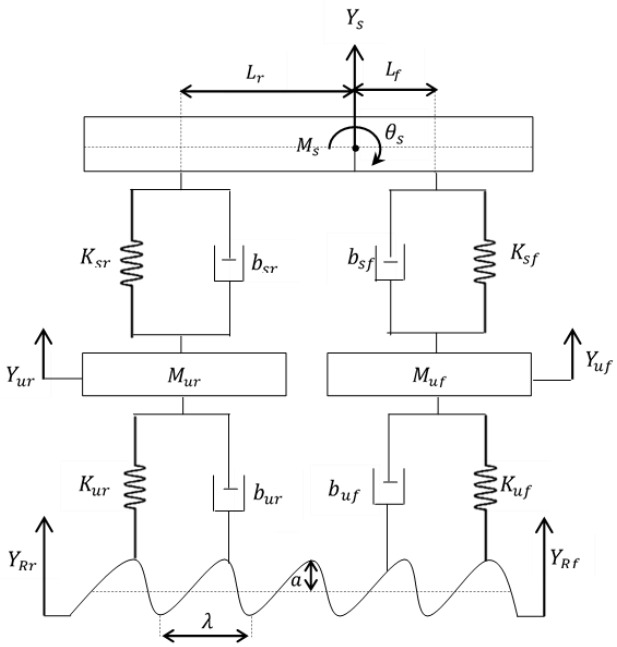

Figure 1. Mechanical system of half car model

Electrical System

The harvester used in this work is a piezoelectric stack that is made of numbers of piezoelectric sheets layers, n, placed on top of each other. These layers are connected mechanically in series and electrically in parallel, which means that each layer will have the same voltage [34]. The piezoelectric stack is operated in 33 mode where the mechanical force is applied along the polarization axis while the electric charge is collected on the surface perpendicular to the polarization axis, as shown in Figure 2.

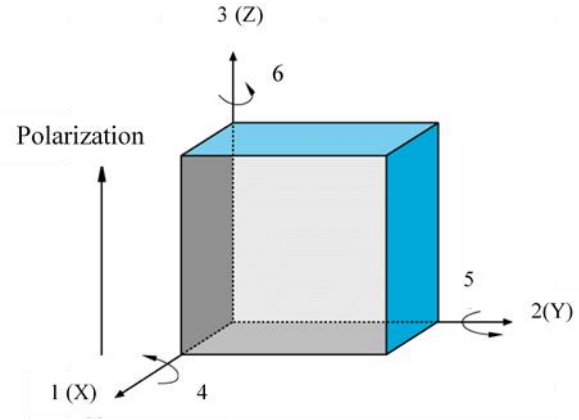

Figure 2. Direction of polarization for a piezoelectric material

In this model, the piezoelectric stack element will be connected in series with the front/rear sprung stiffness in order to not affecting the mechanical performance of the suspension system. Connecting a piezoelectric stack in parallel connection with the suspension spring will increase the equivalent suspension system stiffness and consequently affect the ride quality and comfortability. The equivalent stiffness in the series connection will be approximately equal to the stiffness of the sprung mass as if there is no piezoelectric stack as shown in Figure 3.

Series connection

$$K_{eq} = \frac{K_p + K_s}{K_p K_s} \approx K_s$$

Parallel connection

$$K_{eq} = K_p + K_s$$

Figure 3. Equivalent stiffness as (a) series connection and (b) parallel connection

The piezoelectric material is expressed mathematically as a resorting force in the piezoelectric stack element and the output current from the piezoelectric material (i_p). The restoring force in equation (6) consists of the mechanical and electrical forces with neglecting the effect of piezoelectric damping. The electric circuit is included in order to collect and store the energy converted from the vibration energy. The integrated circuit shown in Figure 4 composed of the piezoelectric material that is modelled as a piezoelectric capacitance (C_p) and resistance (R_p) with the output AC voltage (V_p) connected to the external circuit. The external rectifier circuit consists of the bridge rectifier made of four ideal silicon diodes to obtain the output DC voltage (V) connected to the smoothing capacitor (C_p) and external load (R_e). The smoothing capacitor is utilized to reduce the ripple of the output AC-DC signal.

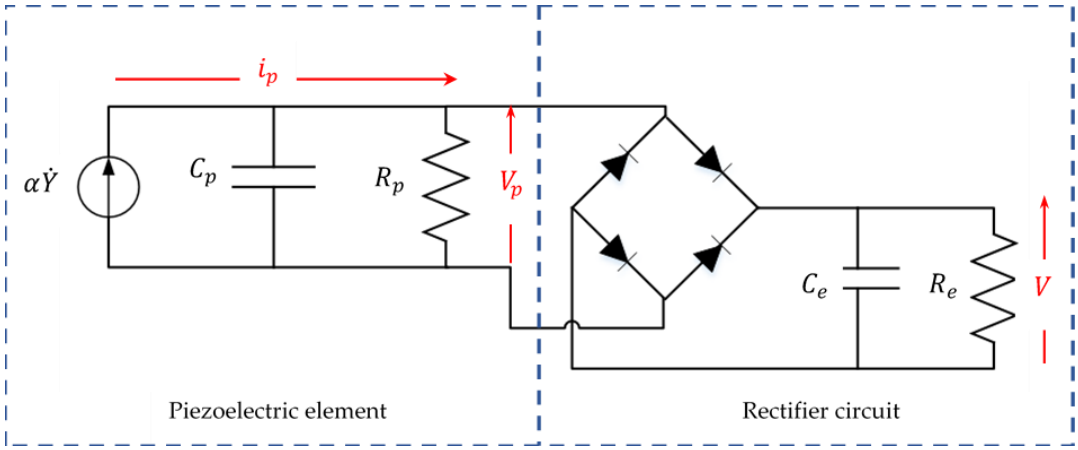

Figure 4. Piezoelectric harvesting circuit

For the piezoelectric element, the relationship between the electrical and mechanical variables can be derived as follows [35]:

$$F_p = K_p Y_p(t) + \alpha V_p(t) \tag{6}$$

$$i_p = \alpha \dot{Y}_p - C_p \dot{V}_p \tag{7}$$

In which the featuring quantities are the short circuit stiffness of piezoelectric stack material K_p, the displacement Y_p, and the force factor α. The mathematical expression of these quantities illustrated in equations (8-10) which are defined as a function of the piezoelectric parameters presented in Table 1.

$$K_p = \frac{E_p A_p}{l_p} \tag{8}$$

$$\alpha = d_{33} E_p \frac{A_p}{t_p} \tag{9}$$

$$C_p = n \frac{\varepsilon_{33} A_p}{t_p} \tag{10}$$

where A_p and t_p are the surface area and thickness of one layer of the piezoelectric stack and the total length of the stack is defined by

$$l_p = n t_p \tag{11}$$

Table 1. Piezoelectric parameters [36]

Parameter	Value	Unit
E_p	53	GPa
d_{33}	630	pm/V
ε_{33}	30.975	nF/m

When a piezoelectric voltage is equal to the output rectified voltage, the diodes conduct, and the current i_p flows from the piezo stack into the external rectifier circuit that can be identified as

$$i_p = \begin{cases} C_e \dot{V} + \dfrac{V}{R_e} & if\ V_p = V \\ -C_e \dot{V} - \dfrac{V}{R_e} & if\ V_p = -V \\ 0 & if\ |V_p| < V \end{cases} \tag{12}$$

From piezoelectric harvesting circuit shown in Figure 4, the resistors and capacitors are connected in parallel. The piezoelectric resistance has a very high value compared to the external load resistance; therefore, the equivalent resistance R is equal to the external resistance $R \approx R_e$. It is also assumed that, the smoothing capacitor C_e is enormous compared to the piezoelectric capacitance C_p, thus the DC rectified voltage is approximated as a constant over a cycle [37, 38]. The equivalent capacitance equals to the piezoelectric capacitance $C \approx C_p$. The external load is modelled as a constant current source, and the four diodes are assumed to exhibit the ideal behavior which means the diode drop is negligible [39]. As a result, the piezoelectric harvesting circuit can be simplified as the equivalent electric circuit as shown in Figure 5 and equation (13) with the values of R =10 kΩ and C = 60 nF.

$$\frac{V}{R} = \alpha \dot{Y}(t) - C \dot{V}(t) \tag{13}$$

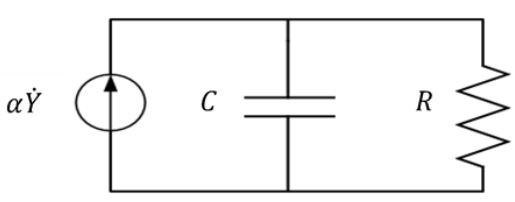

Figure 5. Piezoelectric equivelent circuit

Mechanical System with Piezoelectric Stack

Based on the Newton's second law, the equations of the electromechanical model with built-in piezoelectric stacks mounted in series with the front and rear suspension springs are derived. The derived governing equations can be presented in Laplace transformation as follows:

The equation of bouncing motion of the front unsprung mass:

$$M_{uf}\ddot{Y}_{uf} = -b_{uf}\left(\dot{Y}_{uf} - \dot{Y}_{Rf}\right) - K_{uf}\left(Y_{uf} - Y_{Rf}\right) + b_{sf}\left(\dot{Y}_s - L_f\dot{\theta}_s - \dot{Y}_{uf}\right) + K_{sf}\left(Y_{pf} - Y_{uf}\right) \tag{14}$$

Applying Laplace transformation:

$$\left[M_{uf}s^2 + \left(b_{sf} + b_{tf}\right)s + \left(K_{sf} + K_{tf}\right)\right]Y_{uf} = \left(b_{uf}s + K_{uf}\right)Y_{Rf} + \left(b_{sf}s\right)Y_s - \left(b_{sf}L_fs\right)\theta_s + \left(K_{sf}\right)Y_{pf} \tag{15}$$

The vertical displacement of the front unsprung mass can be written as:

$$Y_{uf} = A_1Y_{Rf} + A_2Y_s - A_3\theta_s + A_4Y_{pf} \tag{16}$$

where

$$A_1 = \left[\frac{b_{uf}s + K_{uf}}{M_{uf}s^2 + \left(b_{sf} + b_{tf}\right)s + \left(K_{sf} + K_{tf}\right)}\right] \qquad A_2 = \left[\frac{b_{sf}s}{M_{uf}s^2 + \left(b_{sf} + b_{tf}\right)s + \left(K_{sf} + K_{tf}\right)}\right]$$

$$A_3 = \left[\frac{b_{sf}L_fs}{M_{uf}s^2 + \left(b_{sf} + b_{tf}\right)s + \left(K_{sf} + K_{tf}\right)}\right] \qquad A_4 = \left[\frac{K_{sf}}{M_{uf}s^2 + \left(b_{sf} + b_{tf}\right)s + \left(K_{sf} + K_{tf}\right)}\right]$$

The equation of bouncing motion of the rear unsprung mass:

$$M_{ur}\ddot{Y}_{ur} = -b_{ur}\left(\dot{Y}_{ur} - \dot{Y}_{Rr}\right) - K_{ur}(Y_{ur} - Y_{Rr}) + b_{sr}\left(\dot{Y}_s + L_r\dot{\theta}_s - \dot{Y}_{ur}\right) + K_{sr}\left(Y_{pr} - Y_{ur}\right) \tag{17}$$

Applying Laplace transformation:

$$\left(M_{ur}s^2 + (b_{sr} + b_{ur})s + (K_{sr} + K_{ur})\right)Y_{ur} = (b_{ur}s + K_{ur})Y_{Rr} + (b_{sr}L_rs)\theta_s + (K_{sr})Y_{pr} + (b_{sr}s)Y_s \tag{18}$$

The vertical displacement of the rear unsprung mass can be written as:

$$Y_{ur} = A_5Y_{Rr} + A_6\theta_s + A_7Y_{pr} + A_8Y_s \tag{19}$$

where

$$A_5 = \left[\frac{b_{ur}s + K_{ur}}{M_{ur}s^2 + (b_{sr} + b_{ur})s + (K_{sr} + K_{ur})}\right] \qquad A_6 = \left[\frac{b_{sr}L_rs}{M_{ur}s^2 + (b_{sr} + b_{ur})s + (K_{sr} + K_{ur})}\right]$$

$$A_7 = \left[\frac{K_{sr}}{M_{ur}s^2 + (b_{sr} + b_{ur})s + (K_{sr} + K_{ur})}\right] \qquad A_8 = \left[\frac{b_{sr}s}{M_{uf}s^2 + \left(b_{sf} + b_{tf}\right)s + \left(K_{sf} + K_{tf}\right)}\right]$$

The equation of bouncing motion of the half-sprung mass:

$$\begin{aligned} M_s\ddot{Y}_s = {} & -b_{sf}\left(\dot{Y}_s - L_f\dot{\theta}_s - \dot{Y}_{uf}\right) - b_{sr}\left(\dot{Y}_s + L_r\dot{\theta}_s - \dot{Y}_{ur}\right) - K_{pf}\left(Y_s - L_f\theta_s - Y_{pf}\right) \\ & - K_{pr}\left(Y_s + L_r\theta_s - Y_{pr}\right) - (\alpha)V_{pf} - (\alpha)V_{pr} \end{aligned} \tag{20}$$

Applying Laplace transformation:

$$\begin{aligned} & \left(M_ss^2 + \left(b_{sf} + b_{sr}\right)s + \left(K_{pf} + K_{pr}\right)\right)Y_s \\ = {} & \left(\left(b_{sf}L_f - b_{sr}L_r\right)s + \left(K_{pf}L_f - K_{pr}L_r\right)\right)\theta_s + \left(b_{sf}s\right)Y_{uf} + (b_{sr}s)Y_{ur} + \left(K_{pf}\right)Y_{pf} \\ & + \left(K_{pr}\right)Y_{pr} - (\alpha)V_{pf} - (\alpha)V_{pr} \end{aligned} \tag{21}$$

The vertical displacement of the sprung mass can be written as:

$$Y_s = A_9\theta_s + A_{10}Y_{uf} + A_{11}Y_{ur} + A_{12}Y_{pf} + A_{13}Y_{pr} - A_{14}V_{pf} - A_{14}V_{pr} \tag{22}$$

where,

$$A_9 = \left[\frac{\left(b_{sf}L_f - b_{sr}L_r\right)s + \left(K_{pf}L_f - K_{pr}L_r\right)}{M_ss^2 + \left(b_{sf} + b_{sr}\right)s + \left(K_{pf} + K_{pr}\right)}\right] \qquad A_{10} = \left[\frac{b_{sf}s}{M_ss^2 + \left(b_{sf} + b_{sr}\right)s + \left(K_{pf} + K_{pr}\right)}\right]$$

$$A_{11} = \left[\frac{b_{sr}s}{M_ss^2 + \left(b_{sf} + b_{sr}\right)s + \left(K_{pf} + K_{pr}\right)}\right] \qquad A_{12} = \left[\frac{K_{pf}}{M_ss^2 + \left(b_{sf} + b_{sr}\right)s + \left(K_{pf} + K_{pr}\right)}\right]$$

$$A_{13} = \left[\frac{K_{pr}}{M_s s^2 + (b_{sf} + b_{sr})s + (K_{pf} + K_{pr})}\right] \qquad A_{14} = \left[\frac{\alpha}{M_s s^2 + (b_{sf} + b_{sr})s + (K_{pf} + K_{pr})}\right]$$

The equation of pitching motion of the half-sprung mass:

$$\begin{aligned} I_s\ddot{\theta}_s = {} & L_f\left(b_{sf}\left(\dot{Y}_s - L_f\dot{\theta}_s - \dot{Y}_{uf}\right) + K_{pf}\left(Y_s - L_f\theta_s - Y_{pf}\right) + \alpha V_{pf}\right) - L_r\left(b_{sr}\left(\dot{Y}_s + L_r\dot{\theta}_s - \dot{Y}_{ur}\right)\right. \\ & \left. + K_{pr}\left(Y_s + L_r\theta_s - Y_{pr}\right) + \alpha V_{pr}\right) \end{aligned} \tag{23}$$

Applying Laplace transformation:

$$\begin{aligned} & \left(I_s s^2 + \left(b_{sf}L_f^2 + b_{sr}L_r^2\right)s + \left(K_{pf}L_f^2 + K_{pr}L_r^2\right)\right)\theta_s \\ & = \left(\left(b_{sf}L_f - b_{sr}L_r\right)s + \left(K_{pf}L_f - K_{pr}L_r\right)\right)Y_s - \left(b_{sf}L_f s\right)Y_{uf} + \left(b_{sr}L_r s\right)Y_{ur} \\ & - \left(K_{pf}L_f\right)Y_{pf} + \left(K_{pr}L_r\right)Y_{pr} + \left(\alpha L_f\right)V_{pf} - \left(\alpha L_r\right)V_{pr} \end{aligned} \tag{24}$$

The angular displacement of the sprung mass can be written as:

$$\theta_s = A_{15}Y_s - A_{16}Y_{uf} + A_{17}Y_{ur} - A_{18}Y_{pf} + A_{19}Y_{pr} + A_{20}V_{pf} - A_{21}V_{pr} \tag{25}$$

where,

$$A_{15} = \left[\frac{\left(b_{sf}L_f - b_{sr}L_r\right)s + \left(K_{pf}L_f - K_{pr}L_r\right)}{I_s s^2 + \left(b_{sf}L_f^2 + b_{sr}L_r^2\right)s + \left(K_{pf}L_f^2 + K_{pr}L_r^2\right)}\right] \qquad A_{16} = \left[\frac{b_{sf}L_f s}{I_s s^2 + \left(b_{sf}L_f^2 + b_{sr}L_r^2\right)s + \left(K_{pf}L_f^2 + K_{pr}L_r^2\right)}\right]$$

$$A_{17} = \left[\frac{b_{sr}L_r s}{I_s s^2 + \left(b_{sf}L_f^2 + b_{sr}L_r^2\right)s + \left(K_{pf}L_f^2 + K_{pr}L_r^2\right)}\right] \qquad A_{18} = \left[\frac{K_{pf}L_f}{I_s s^2 + \left(b_{sf}L_f^2 + b_{sr}L_r^2\right)s + \left(K_{pf}L_f^2 + K_{pr}L_r^2\right)}\right]$$

$$A_{19} = \left[\frac{K_{pr}L_r}{I_s s^2 + \left(b_{sf}L_f^2 + b_{sr}L_r^2\right)s + \left(K_{pf}L_f^2 + K_{pr}L_r^2\right)}\right] \qquad A_{20} = \left[\frac{\alpha L_f}{I_s s^2 + \left(b_{sf}L_f^2 + b_{sr}L_r^2\right)s + \left(K_{pf}L_f^2 + K_{pr}L_r^2\right)}\right]$$

$$A_{21} = \left[\frac{\alpha L_r}{I_s s^2 + \left(b_{sf}L_f^2 + b_{sr}L_r^2\right)s + \left(K_{pf}L_f^2 + K_{pr}L_r^2\right)}\right]$$

The mechanical and electrical relationships in equation (6) will be modified for the front and rear piezoelectric stacks as

Front piezoelectric stack:

$$M_{pf}\ddot{Y}_{pf} = -K_{sf}\left(Y_{pf} - Y_{uf}\right) + K_{pf}\left(Y_s - L_f\theta_s - Y_{pf}\right) + (\alpha)V_{pf} \tag{26}$$

Applying Laplace transformation:

$$\left(M_{pf}s^2 + \left(K_{sf} + K_{pf}\right)\right)Y_{pf} = \left(K_{sf}\right)Y_{uf} + \left(K_{pf}\right)Y_s - \left(K_{pf}L_f\right)\theta_s + (\alpha)V_{pf} \tag{27}$$

The vertical displacement of the front piezoelectric stack can be written as

$$Y_{pf} = A_{22}Y_{uf} + A_{23}Y_s - A_{24}\theta_s + A_{25}V_{pf} \tag{28}$$

where,

$$A_{22} = \left[\frac{K_{sf}}{M_{pf}s^2 + \left(K_{sf} + K_{pf}\right)}\right] \qquad A_{23} = \left[\frac{K_{pf}}{M_{pf}s^2 + \left(K_{sf} + K_{pf}\right)}\right]$$

$$A_{24} = \left[\frac{K_{pf}L_f}{M_{pf}s^2 + \left(K_{sf} + K_{pf}\right)}\right] \qquad A_{25} = \left[\frac{\alpha}{M_{pf}s^2 + \left(K_{sf} + K_{pf}\right)}\right]$$

Rear piezoelectric stack:

$$M_{pr}\ddot{Y}_{pr} = -K_{sr}\left(Y_{pr} - Y_{ur}\right) + K_{pr}\left(Y_s + L_r\theta_s - Y_{pr}\right) + (\alpha)V_{pr} \tag{29}$$

Applying Laplace transformation:

$$\left(M_{pr}s^2 + \left(K_{sr} + K_{pr}\right)\right)Y_{pr} = \left(K_{sr}\right)Y_{ur} + \left(K_{pr}\right)Y_s + \left(K_{pr}L_r\right)\theta_s + (\alpha)V_{pr} \tag{30}$$

The vertical displacement of the rear piezoelectric stack can be written as

$$Y_{pr} = A_{26}Y_{ur} + A_{27}Y_s + A_{28}\theta_s + A_{29}V_{pr} \tag{31}$$

where,

$$A_{26} = \left[\frac{K_{sr}}{M_{pr}s^2 + \left(K_{sr} + K_{pr}\right)}\right] \qquad A_{27} = \left[\frac{K_{pr}}{M_{pr}s^2 + \left(K_{sr} + K_{pr}\right)}\right]$$

$$A_{28} = \left[\frac{K_{pr}L_r}{M_{pr}s^2 + (K_{sr} + K_{pr})}\right] \qquad A_{29} = \left[\frac{\alpha}{M_{pf}s^2 + (K_{sf} + K_{pf})}\right]$$

The governing equations for the equivalent electrical system as derived in equation (13) can be modified and written separately in Laplace transformation as:

The front harvested voltage and power:

$$V_f = \alpha R(\dot{Y}_s - L_f\dot{\theta}_s - \dot{Y}_{pf}) - CR\dot{V}_f \tag{32}$$

Applying Laplace transformation:

$$V_f = A_{30}Y_s - A_{31}\theta_s - A_{30}Y_{pf} \tag{33}$$

$$P_f = \frac{V_f^2}{R} \tag{34}$$

The rear harvested voltage and power:

$$V_r = \alpha R(\dot{Y}_s + L_r\dot{\theta}_s - \dot{Y}_{pr}) - CR\dot{V}_r \tag{35}$$

Applying Laplace transformation:

$$V_r = A_{30}Y_s + A_{32}\theta_s - A_{30}Y_{pr} \tag{36}$$

$$P_r = \frac{V_r^2}{R} \tag{37}$$

where

$$A_{30} = \frac{\alpha Rs}{CRs + 1} \qquad A_{31} = \frac{L_f\alpha Rs}{CRs + 1} \qquad A_{32} = \frac{L_r\alpha Rs}{CRs + 1}$$

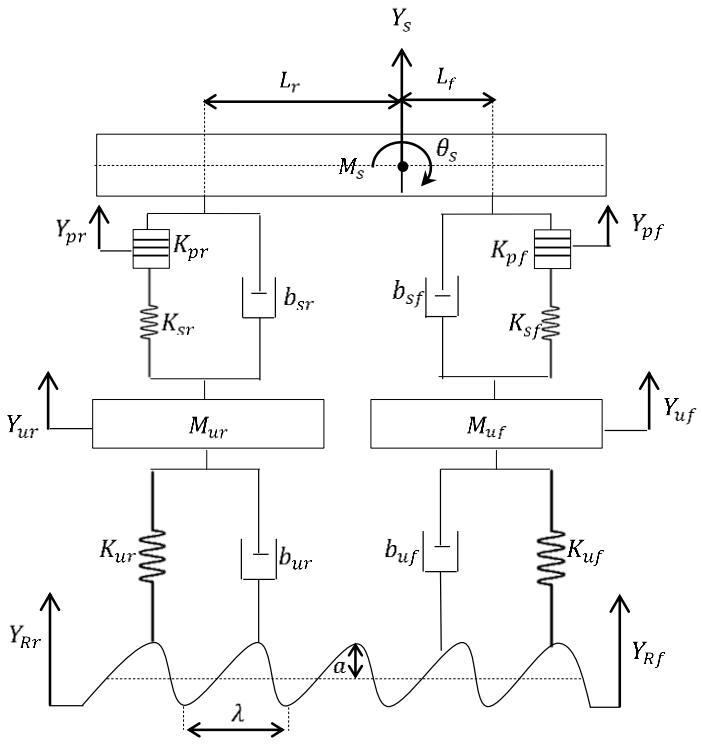

Figure 6. Energy harvesting model

RESULTS AND DISCUSSION

In order to evaluate the harvested power from a half car model using piezoelectric harvesting system, MATLAB/Simulink model demonstrated in Figure 7 is built to carry out the time and frequency domains simulation for the performance of the proposed harvesting system. The suspension parameters used in the mathematical model are listed in Table 2 [40].

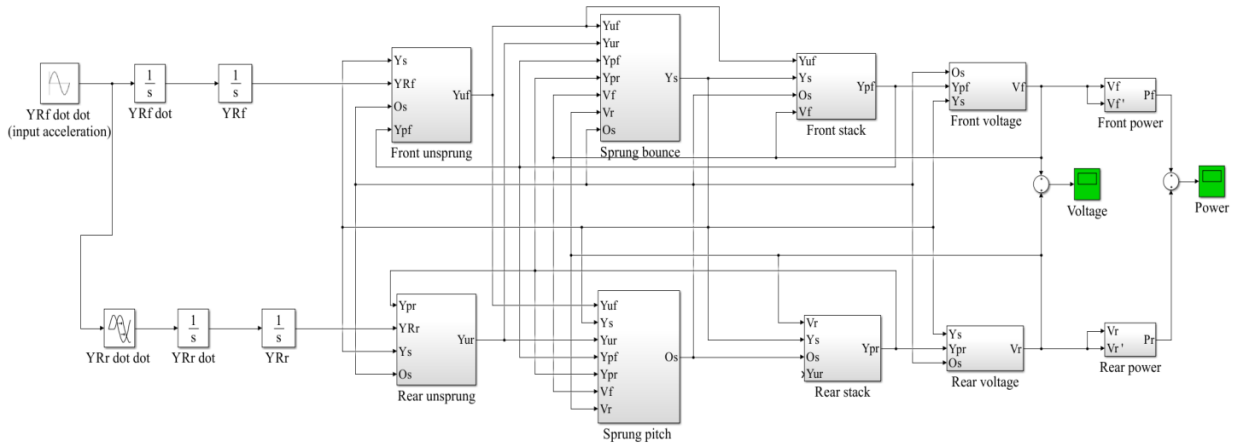

Figure 7. Simulation scheme for the energy harvesting model

Table 2. Parameters used in the mathematical model of the half car suspension system [40, 41]

Parameter	Value	Unit
M_s	520	kg
M_{uf}, M_{ur}	40	kg
I_s	2000	kgm^2
K_f, K_r	26000	N/m
Kt_f, Kt_r	130000	N/m
C_f, C_r	520	Ns/m
Ct_f, Ct_r	265.73	Ns/m
L_f	1.23	M
L_r	1.65	m

Calculating the natural frequencies of any harmonic excitation model is essential to define the locations of the resonance. Since half car model is four degrees of freedom (4 DOF), this means that it has four natural frequencies that can be found from the peak values of the displacement amplitude of each sub-system with the input road displacement amplitude as shown in Figure 8.

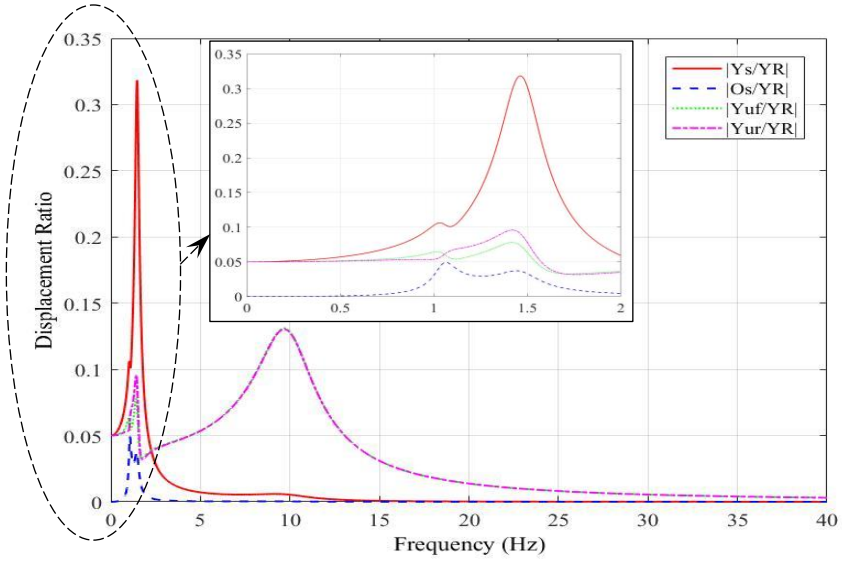

Figure 8. Displacement ratio vs. frequency for 4 DOF model

Piezoelectric stack of type PZT-5H is utilized in this study due to its advantages in harvesting the vibration loss energy. It is widely available that makes it cheap, and it has a high value of piezoelectric constant d_{33} [42]. Two piezoelectric stacks are mounted in series with the front and rear suspension's springs in the half car model. Therefore, their series mounting will not affect the dynamic performance of the suspension system. The recommended natural frequency of the sprung mass is below 1.5Hz. A value of more than 1.5Hz is not expected since it increases the acceleration of the car body and causes discomfort to the passengers. Also, the natural frequency of the pitch mode should be close to the bounce mode of the sprung mass and should not be affected during the pitch motion. Moreover, the unsprung masses natural frequencies should be not less than 8Hz since the human body is more sensitive to the vertical vibration motion in the frequency range of 4-8Hz. The natural frequencies of the energy harvesting system presented in Table 3 match the ranges that are recommended by Hossain and Chowdhury [43].

Table 3. Natural frequencies of the half car model

Description	f (Hz)
Sprung pitch motion	1.06
Sprung bounce motion	1.46
Front unsprung bounce motion	9.68
Rear unsprung bounce motion	9.68

The available harvesting power from vehicles subjected to harmonic excitation is the amount of the power dissipated by the suspension dampers. Thus, the average potential power from the front and rear suspension dampers in one oscillation is the product of the damping force and its relative velocity which can be calculated as [44]:

$$P_{avg} = \frac{b_{sf}\omega^2\left(Y_s - L_f\theta - Y_{uf}\right)^2}{2} + \frac{b_{sr}\omega^2(Y_s + L_r\theta - Y_{ur})^2}{2} \tag{38}$$

where (Y_s - L_f θ - Y_{uf}) and (Y_s + L_r θ - Y_{ur}) are the amplitude of the relative displacement of the suspension. The average power by the suspension dampers in the frequency domain is depicted in Figure 9. The peak values of power dissipated from the suspension dampers are occurred at the resonant frequencies of the system. At the pitch natural frequency, the dissipated power is about 187W.

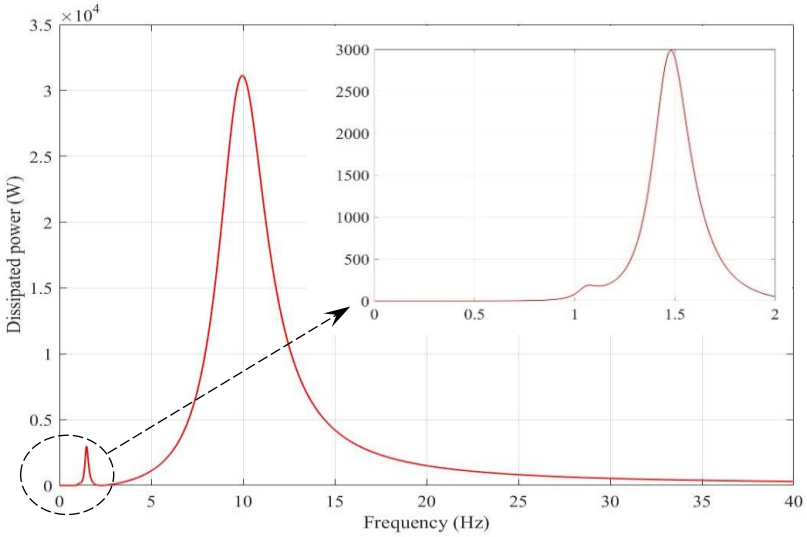

Figure 9. The variation of the average dissipated power by the suspension dampers in the frequency domain

The road texture is divided into four main groups according to the ISO 13473-1 [45]. The value of the texture wavelength λ for each category is i- microtexture: λ < 0.5mm, ii- macrotexture: 0.5mm < λ < 50mm, iii- megatexture: 50mm < λ < 0.5m and iv- unevenness: 0.5m < λ < 50m. The common unevenness texture wavelength used in the literature is 5m [46]. The vehicle traveling velocity u over a road is affected by the excitation frequency f and the road wavelength λ as shown in the following equation,

$$u = f\lambda \tag{39}$$

Since most of the vehicles' rigid body excitation frequency within the range [0.5 - 15Hz], so that the corresponding vehicle velocity is varied between 9km/h and 270km/h [47]. Accordingly, the results from Figure 10 showed that, the first dissipated power occurs when the vehicle is traveled at a velocity of 19km/h. The second corresponding peak that reveals to the sprung bouncing mode has a power dissipation of 2990W. However, the average power increases significantly to 31kW at the front and rear unsprung natural frequency of 9.7Hz with a velocity of 174.24km/h.

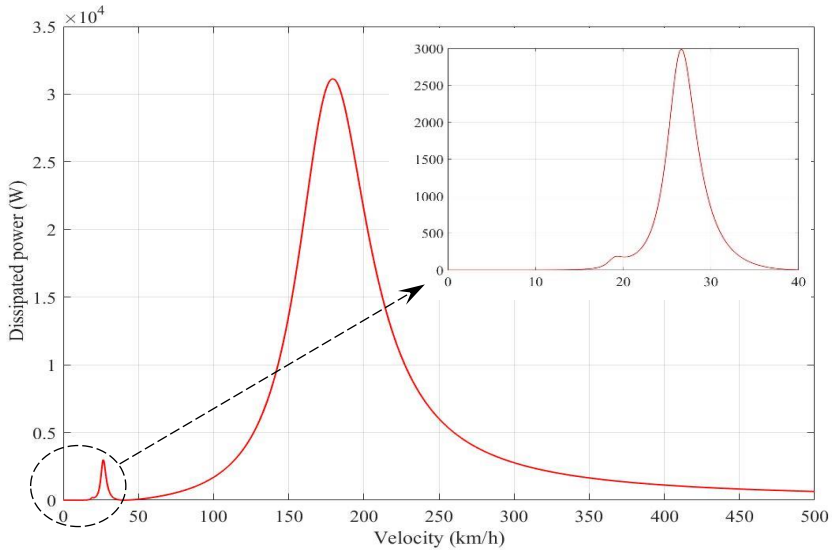

Figure 10. The variation of the average dissipated power by the suspension dampers with different car velocities

Harvesting the potential power from car suspension system is carried out by inserting two piezoelectric stacks each has 40 layers with a surface area and length of 49mm^2 and 40mm, respectively. The steady-state responses for evaluating the harvested voltage and power are simulated by exciting the vehicle using sinusoidal acceleration excitation input with an amplitude of 0.5g (4.9m/s^2) and velocity of 9.17rad/s. It can be observed from Figure 11 that, the maximum generated voltage and power at the steady state phase are around 33.51V and 56.25mW, respectively. The root mean square RMS for the harmonic excitation of the harvested voltage and power are 23.7V and 28.13mW, respectively.

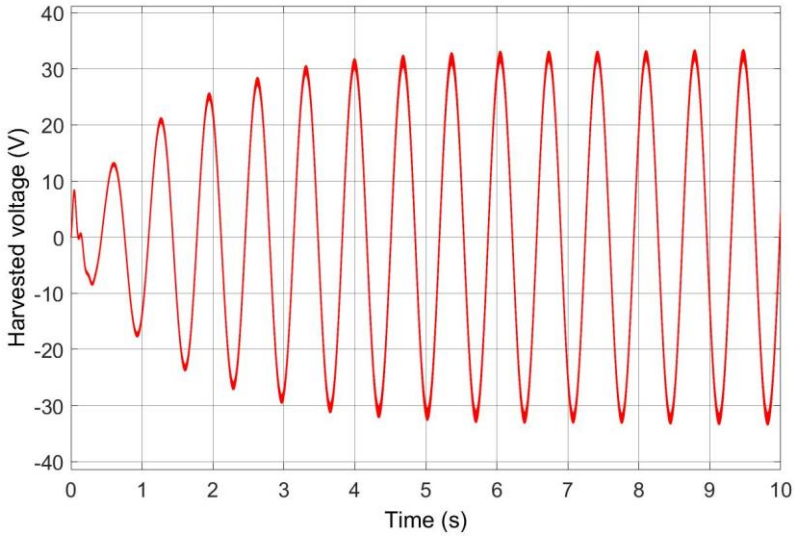

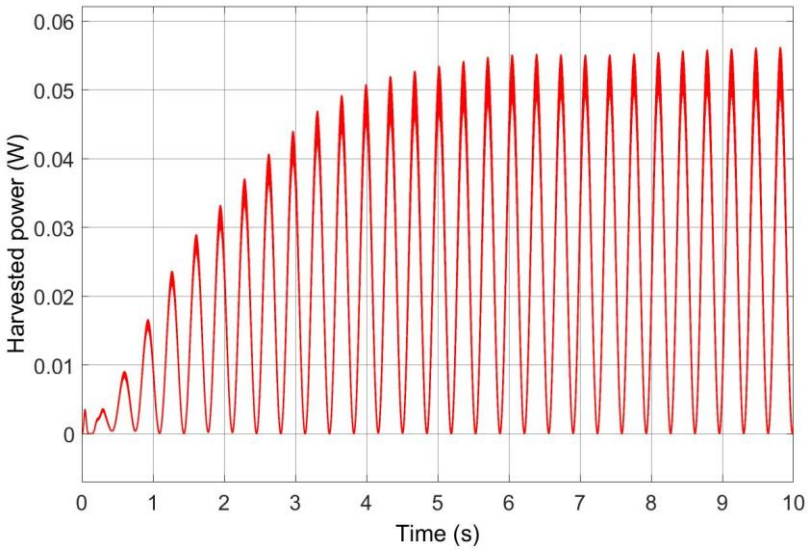

Figure 11. Harvested voltage and power in the time domain

The harvested voltage and power were also studied in the frequency domain, as demonstrated in Figure 12. The input excitation frequency was varied from 0 to 20Hz, and the other car's parameters were kept fixed. The results show that, the first peak occurs at the sprung pitch natural frequency with the output voltage and power values of 17.82V and 31.74mW, respectively. While the second peak records at the sprung bounce natural frequency of 1.46Hz, which has a corresponding harvested voltage of 33.51V and power of 56.25mW. For the front and rear unsprung natural frequencies (f = 9.68Hz), the output voltage and power are recorded as 2.815V and 0.39mW, respectively. Thus, it can be concluded, as expected, that, at the resonant frequencies, more harvested energy is generated if compared with that of the non-resonant frequencies.

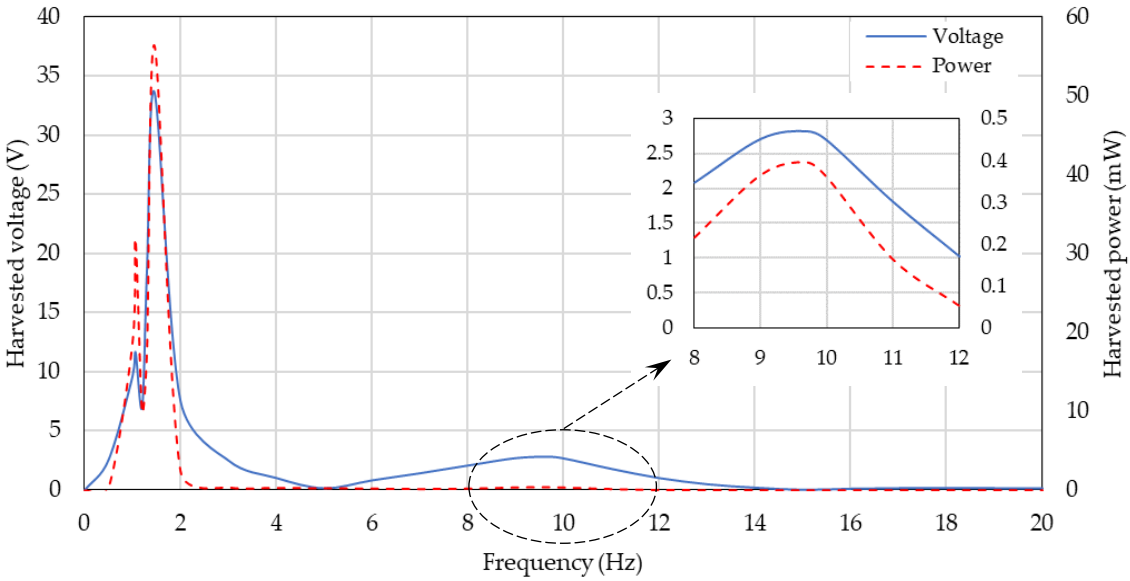

Figure 12. Harvested voltage and power in the frequency domain

The harvested voltage and power at different vehicle velocities are also demonstrated in Figure 13. It can be pointed out that, the trend of variation of the harvested voltage and power versus frequency (Figure 12) is similar to that of the harvested voltage and power versus car velocity (Figure 13). The reason behind this similarity is that, the frequency and velocity are directly proportional to each other. This correlation is illustrated in equation (39) at a road wavelength λ of 5m. The maximum values take place at the velocities corresponding to the resonant frequencies. Accordingly, the most significant output voltage and power occur at velocity of 26.28km/h that corresponds to the sprung bounce natural frequency of 1.46Hz. While at the excitation frequency of 1.06Hz, the corresponding vehicle velocity is found to be 19.1km/h that can provide harvested voltage and power of 11.63V and 31.74mW, respectively. The lowest peaks of the harvested voltage and power related to the unsprung natural frequency at car velocity of 174.24km/h.

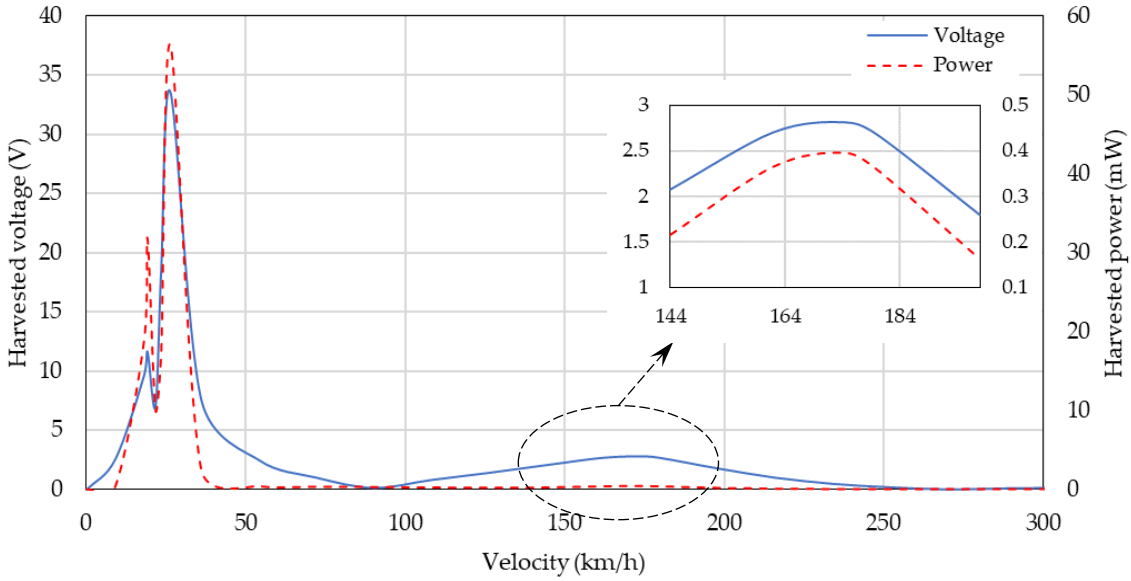

Figure 13. Harvested voltage and power in different vehicle velocities

Taking the most common velocity ranges where the vehicles usually run [40 – 100km/h], the harvested voltage and power is calculated as presented in Figure 14. This velocity ranges correspond to the non-resonance frequencies. It can be noticed that the harvested voltage and power decrease with velocity from 5.5V to 0.5V and 1.5mW to 0.24mW, respectively. Also, the harvested voltage and power at 40 km/h (5.5 V and 1.515 mW) are more than the power harvested at the unsprung bounce resonant frequency (2.82V and 0.39mW). This illustrates that yet the system can harvest power out of the resonant frequencies and within the most suitable velocity range at which the vehicles move. For instance, if the car travelled from Abu Dhabi to Dubai at speed of 110km/h for 2 hours, this would result in harvesting energy of 1.6J.

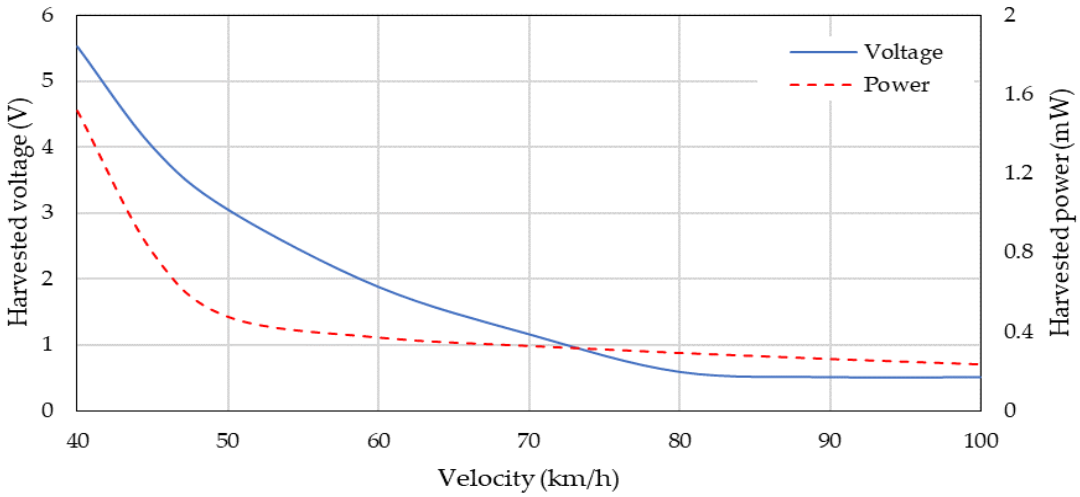

Figure 14. Harvested voltage and power in different vehicle velocities (non-resonance frequency)

The effect of road unevenness acceleration amplitude on the harvested voltage and power at the excitation frequency of 1.46Hz are depicted in Figure 15. The output voltage from the piezoelectric stack increases linearly from 6.7V up to 67.03V with the road acceleration amplitude of 0.1g to 1g. However, the output power rises in a quadratic relationship with minimum and maximum harvested power of 2.25mW and 225mW, respectively. It can be noticed that, the harvested voltage and power increases with the amplitude road unevenness. This is due to the change of the linear momentum of the vehicle, which means an increase of the vehicle velocity and consequently increases the harvested voltage and power with respect to the unevenness amplitude.

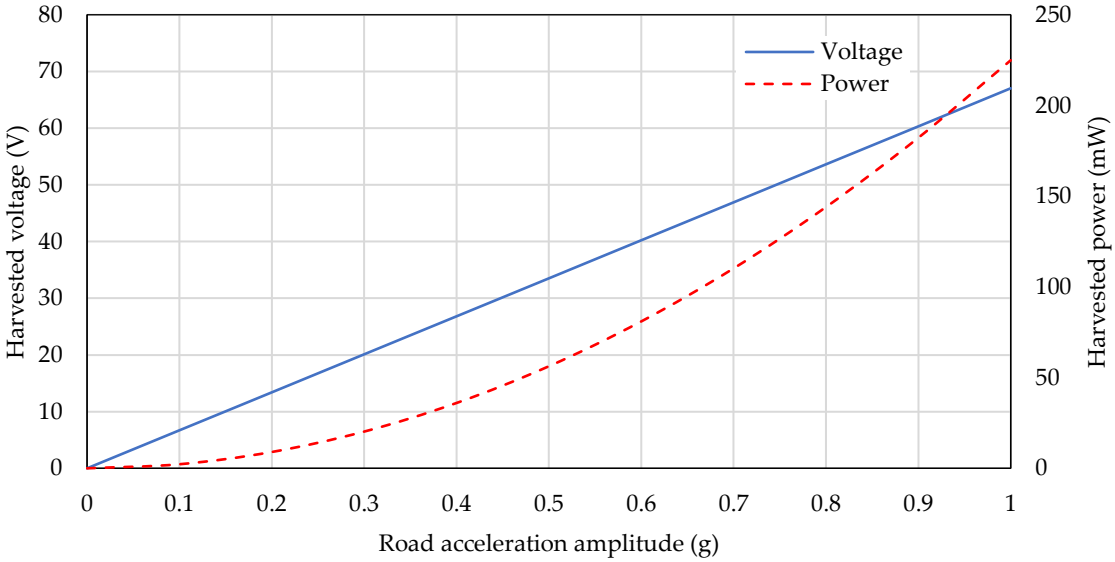

Figure 15. Harvested voltage and power vs. different amplitudes of road unevenness at excitation frequency of 1.46Hz

It can be noted from the previous results that, the harvested power from a proposed energy harvesting system of a half car model with built-in piezoelectric stack cannot be compared with different harvesting systems found in the literature. The energy harvesting systems are diverse in the configuration (cantilever [8–10] and stack [11–14]), location of the piezoelectric element in the suspension system (springs [3–5, 14], shock absorbers [8, 10–13], and wheels [6–8]), the suspension system model (quarter [4, 6, 8, 10, 14] or half car model [5]), and the road input excitation (harmonic [4, 5, 11, 14] or random [6, 8, 10, 12]).

The effect of the piezoelectric stack parameters, such as the number of layers and area/thickness ratio was also investigated on the performance of the energy harvesting model. The study was conducted for a multiple number of layers up to 100 layers. The results demonstrated in Figure 16 show that, having more layers would increase the harvested voltage linearly and the harvested power exponentially. The multiple layers are connected electrically in parallel, therefore, the total displacement of the piezoelectric stack could be expressed according reference [34] as follows,

$$Y_{stack} = nY_p = \frac{1}{K_p}F_p + nd_{33}V \tag{40}$$

According to equation (40), it can be observed that, the overall displacement of the stack increases with the number of layers which will consequently decrease the stiffness of the piezoelectric stack. Besides, the total charge in the piezoelectric stack is the summation of the output charge of all layer. This observation is supported by equation (41). As a result, the output voltage and power from the proposed piezoelectric stack with 40 up to 100 layers increase by 54V and 0.3W.

$$Q_{stack} = nQ_p = nd_{33}f + C_pV \tag{41}$$

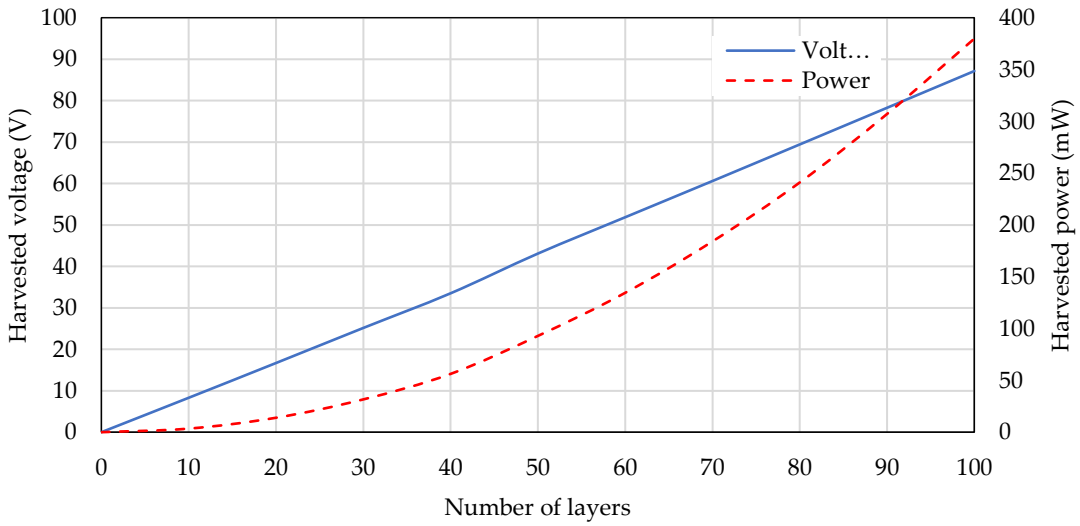

Figure 16. The effect of the number of layers of the piezoelectric stack on the harvested power

Area to thickness ratio is another parameter of the piezoelectric stack that could be studied. Studying this parameter will influence different stack parameters such as the force factor, stiffness, and capacitance of the piezoelectric material. The ratio has been examined within a range of [1-1000]mm. As the ratio increased, the harvested power was also increased by 0.3W (see Figure 17) due to the increase of the electric generating capacity of the piezoelectric stack.

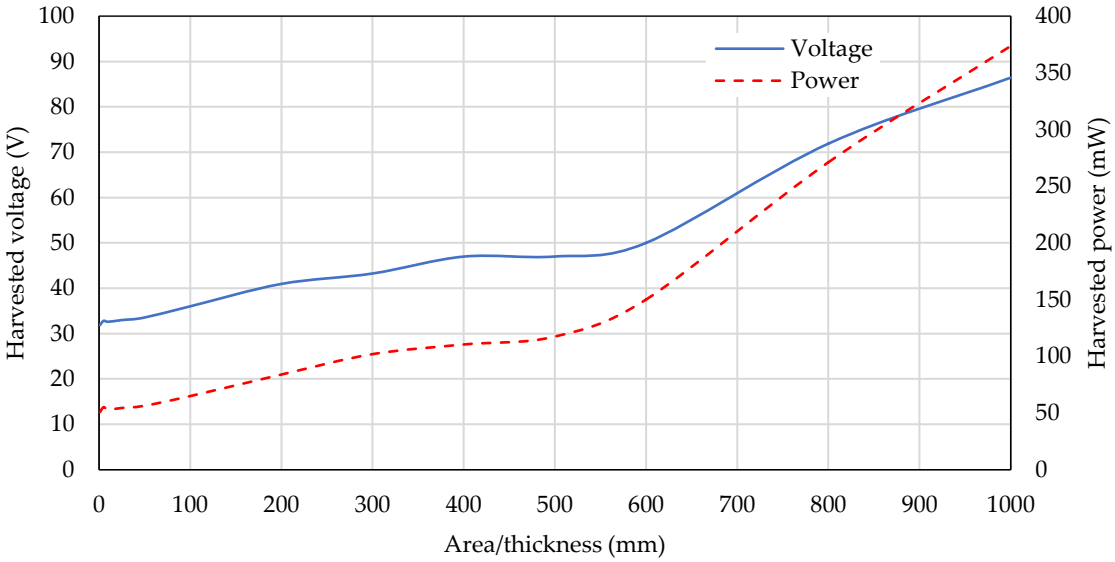

Figure 17. The effect of area/thickness ratio of the piezoelectric stack on the harvested power

The effect of different car parameters on the performance of the half car piezoelectric energy harvesting model was examined as well. Each studied car parameter in Table 2 was changed, and the other unstudied parameters were kept constant. The influence of the sprung and unsprung stiffness coefficient is demonstrated in Figures 18 through 20. The results show that, both the sprung and unsprung resonant frequencies increase with increasing the stiffness coefficient. This result is validated by the relationship between the natural frequencies of the system and the stiffness coefficient constant (i.e., $\omega=\sqrt{K/M}$). In contrast, increasing the tire stiffness will decrease the resonance power which means that, stiffer tires result in a harder ride and less suspension movement. However, increasing the suspension stiffness will increase the relative displacement between the sprung mass and the piezoelectric stack. Accordingly, this will rise the harvested power from the piezoelectric stack as shown in Figures 18.

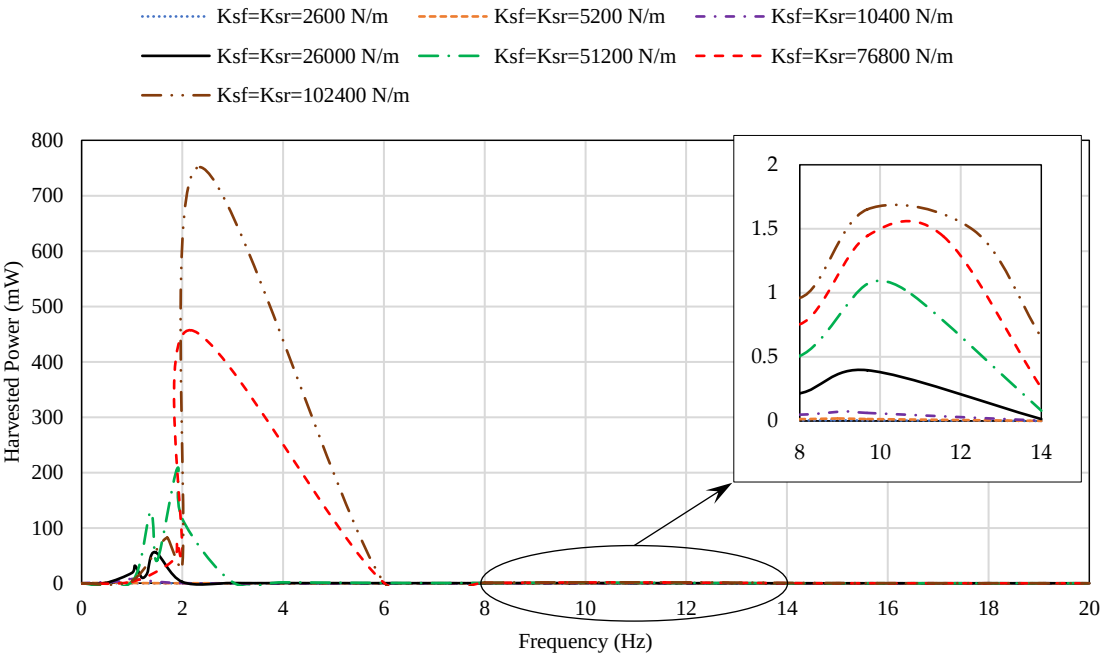

Figure 18. Effect of the sprung stiffness coefficient on the harvested power

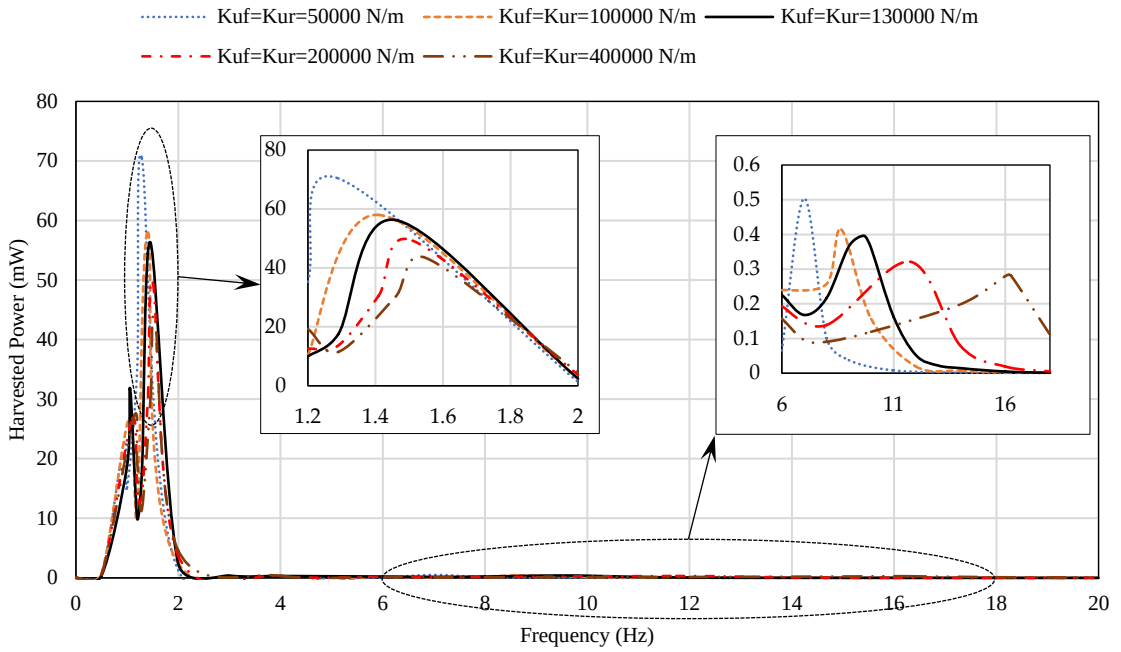

Figure 19. Effect of the unsprung stiffness coefficient on the harvested power

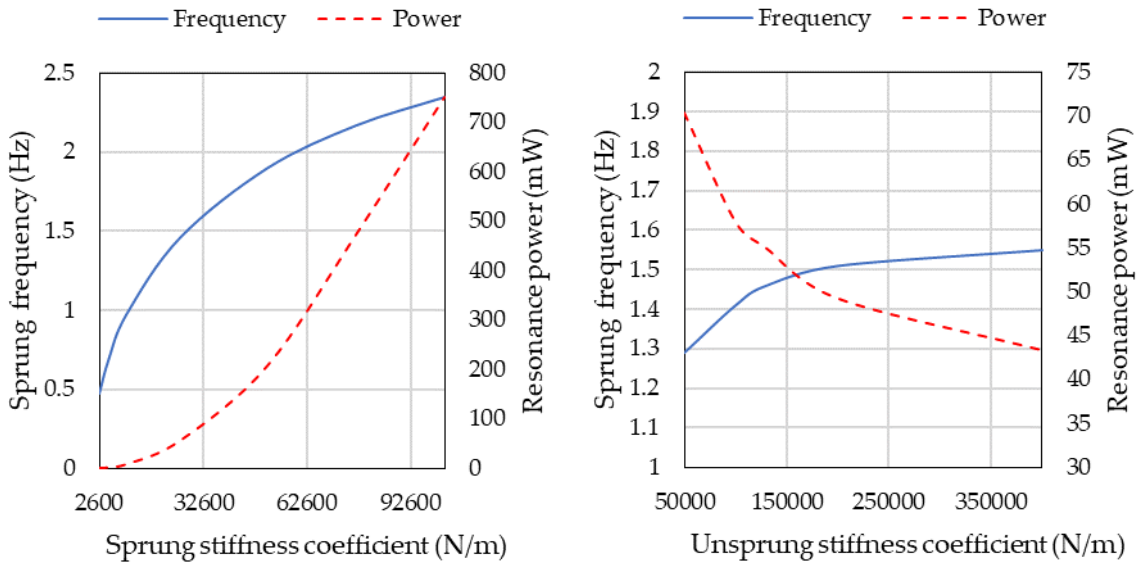

Figure 20. Effect of the sprung and unsprung stiffness coefficient on the output sprung resonant frequency and resonance power

Sprung and unsprung damping coefficients were examined as demonstrated in Figures 21 through 23. The results show that, increasing the damping coefficient for both masses will significantly reduce the output resonance power. However, the sprung resonant frequency will not be affected (see Figure 23). It was also observed that, less suspension damping will provide higher harvested power by allowing more stress to be applied to the piezoelectric material. Conversely, having lightly damped or soft suspension will reduce car handling performance and stability [34, 39].

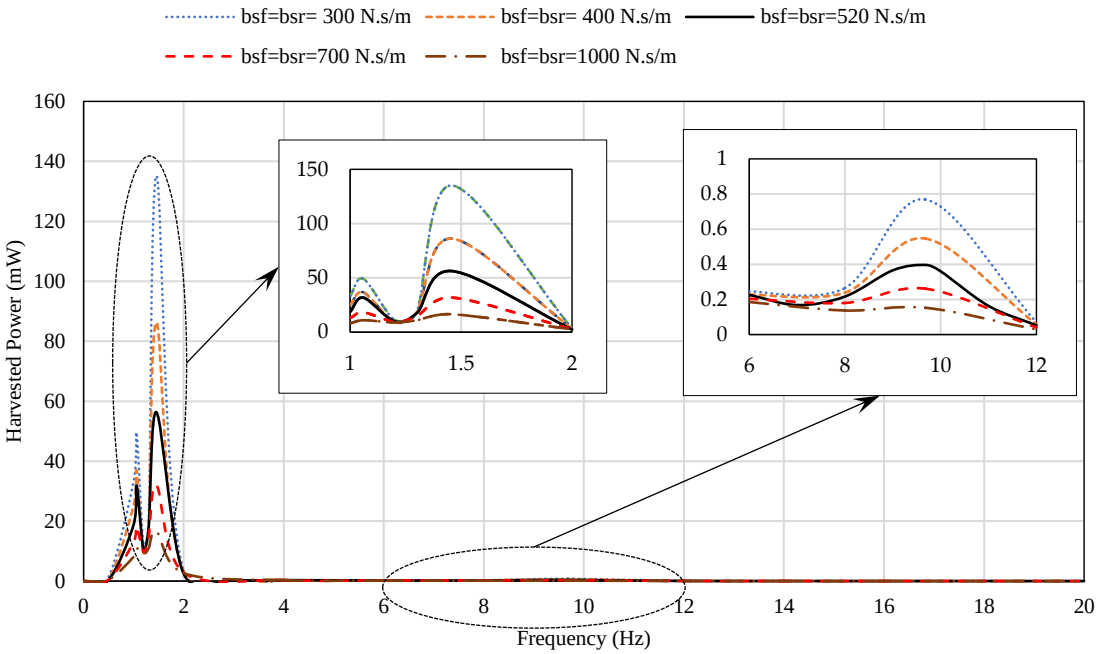

Figure 21. Effect of the sprung damping coefficient on the harvested power

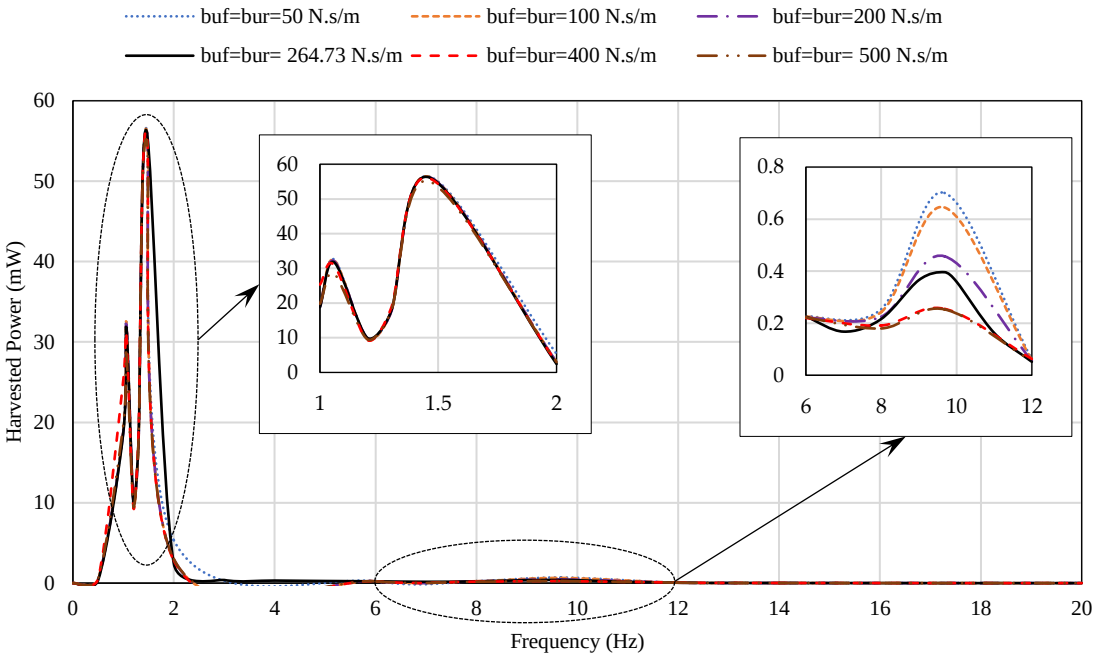

Figure 22. Effect of the unsprung damping coefficient on the harvested power

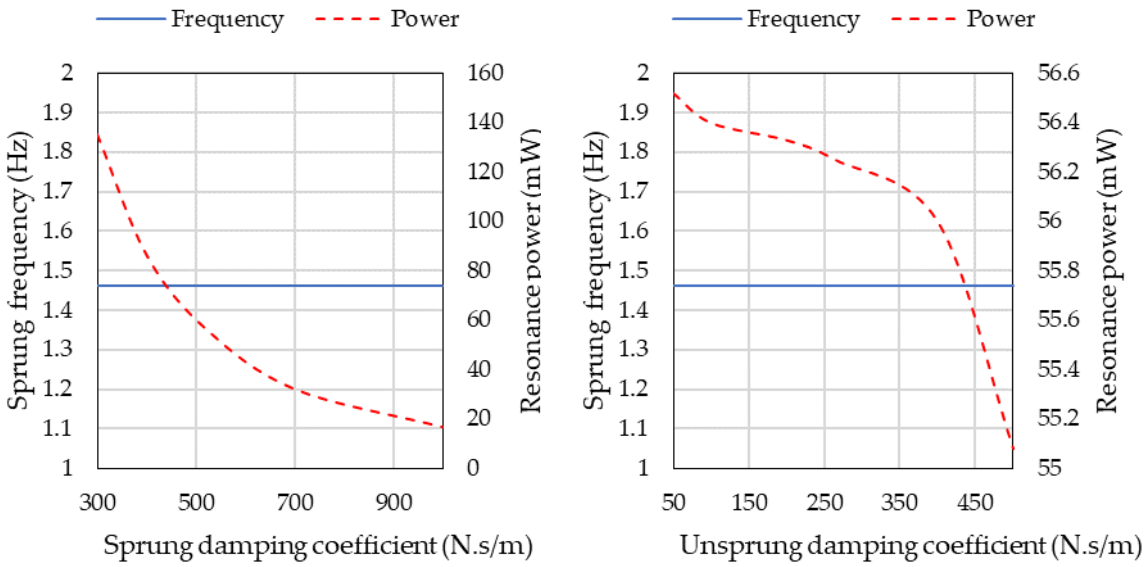

Figure 23. Effect of the sprung/unsprung damping coefficient on the output sprung resonant frequency and a resonance power

The previous findings illustrated that, there is a significant potential for harvesting energy from the car suspension system. The generated vibrations from the road excitation are transmitted to the car suspension system, and the produced stress will be applied to the piezoelectric stack material. The piezoelectric material will be deformed and created a significant amount of an electric charges. Without these harvesters, the vibration energy is wasted and dissipated into heat. Moreover, the vehicle suspension system and piezoelectric stack parameters have shown an essential impact on the amount of harvested energy. However, there are several solutions proposed by Al-Yafeai et al. [49] in order to maximize the harvested power from vehicles. Improved the material properties of the piezoelectric material to be equipped with the car will help in harvesting most of the vibrations subjected to the cars. The configuration of the harvester with the direction of the applied force has a significant impact on the harvested power. For instance, multilayer piezoelectric sheets stacked on top of each other can withstand large mechanical forces that will magnify the output charge when compared to a single layer. Moreover, most of the researchers optimize the output harvested power by connecting the voltage regulator or an inductor to the energy harvesting circuits.

The harvested energy from the vehicles could be directly utilized or stored in a car battery [50–52]. The batteries will be self-charged as the car moves and excited by road irregularities. Accordingly, the battery could be act as an additional electric car battery due to their limited lifetime. The energy harvested batteries could also be utilized in emergency cases to start up the car when it shut off. Besides, the harvested energy could run different wireless sensors and other auxiliary systems in the cars.

CONCLUSIONS

Half car model with built-in piezoelectric stack was modeled mathematically using Laplace transformation. The maximum output voltage and power from the front and rear piezoelectric stacks were generated at the resonant frequencies. The car was excited under harmonic input with a frequency of 1.46Hz and acceleration amplitude of 0.5g results in a voltage of 33.51V and power of 56.25mW. The findings also showed that the system could harvest power out of the resonance frequencies with a remarkable harvested power (1.515mW at 40km/h).

Different factors were tested on evaluating the harvested power from car suspension system. For instance, higher road amplitude results in higher harvested power. Besides, increasing piezoelectric stack parameters such as the number of layers and area to thickness ratio were found to increase the harvested power. Furthermore, the parameters of the car suspension system, such as stiffness and damping coefficients, affect the generated results. Stiffer suspension springs provide higher resonant frequency and higher relative displacement, which results in higher harvested power. However, stiffer tires decrease the harvested power due to the less suspension movement and hard ride. On the other hand, increasing the damping coefficients of the sprung and unsprung systems reduce the harvested power due to minimizing the unwanted vibrations in the suspension system. However, low damping coefficients provide more stresses on the piezoelectric stack, which negatively affects the car handling performance and stability. Therefore, it would be recommended in the future work to determine a balance point between both the car handling performance and the amount of the harvested energy.

ACKNOWLEDGMENTS

The authors would like to acknowledge UAEU-Research Center-ECEER, United Arab Emirates University (UAEU) for research grants and funding.

REFERENCES

[1] K. E. Graves, P. G. Iovenitti, D. Toncich, "Electromagnetic regenerative damping in vehicle suspension systems," *International Journal of Vehicle Design*, vol. 24, no. 2–3, pp. 182–197, 2000.

[2] L. Segel and X. Lu, "Vehicular resistance to motion as influenced by road roughness and highway alignment," *Australian Road Research*, vol. 12, no. 4, pp. 211–222, 1982.

[3] C. S. Namuduri, Y. Li, T. J. Talty, R. B. Elliott, N. Mcmahon, "Harvesting energy from vehicular vibrations using piezoelectric devices," US patent US008143766B2, 2012.

[4] X. Wang, *Frequency analysis of vibration energy harvesting systems*. Academic Press, 2016.

[5] D. Al-Yafeai, T. Darabseh, A-H. I. Mourad, "Quarter vs. Half Car Model Energy Harvesting Systems," in *2019 IEEE Advances in Science and Engineering Technology International Conferences (ASET)*, pp. 1–5, 2019.

[6] X. D. Xie and Q. Wang, "Energy harvesting from a vehicle suspension system," *Energy*, vol. 86, pp. 385–392, 2015.

[7] M. M. Behera, "Piezoelectric Energy Harvesting from Vehicle Wheels," *International Journal of Engineering Research & Technology*, vol. 4, no. 05, 2015.

[8] B. Lafarge, S. Grondel, C. Delebarre, E. Cattan, "A validated simulation of energy harvesting with piezoelectric cantilever beams on a vehicle suspension using Bond Graph approach," *Mechatronics*, vol. 53, pp. 202–214, 2018.

[9] H. Lee, H. Jang, J. Park, S. Jeong, T. Park, S. Choi, "Design of a piezoelectric energy-harvesting shock absorber system for a vehicle," *Integrated Ferroelectrics*, vol. 141, no. 1, pp. 32–44, 2013.

[10] B. Lafarge, C. Delebarre, S. Grondel, O. Curea, and A. Hacala, "Analysis and optimization of a piezoelectric harvester on a car damper," *Physics Procedia* vol. 70, pp. 970–973, 2015.

[11] S. F. Ali and S. Adhikari, "Energy harvesting dynamic vibration absorbers," *Journal of Applied Mechanics*, vol. 80, no. 4, pp. 1-9, 2013.

[12] C. Madhav and S. F. Ali, "Harvesting energy from vibration absorber under random excitations," *IFAC-Pap.*, vol. 49, no. 1, pp. 807–812, 2016.

[13] M. Arizti, "Harvesting energy from vehicle suspension," Master of Science Thesis, Tampere University of Technology, Tampere, 2010.

[14] W. Hendrowati, H. L. Guntur, I. N. Sutantra, "Design, modeling and analysis of implementing a multilayer piezoelectric vibration energy harvesting mechanism in the vehicle suspension," *Engineering*, vol. 4, no. 11, pp. 728-738, 2012.

[15] L. Zuo and P.-S. Zhang, "Energy harvesting, ride comfort, and road handling of regenerative vehicle suspensions," *Journal of Vibration and Acoustics*, vol. 135, no. 1, pp. 295-302, 2013.

[16] Z. Fang, X. Guo, L. Xu, H. Zhang, "An optimal algorithm for energy recovery of hydraulic electromagnetic energy-regenerative shock absorber," *Applied Mathematics & Information Sciences*, vol. 7, no. 6, pp. 2207-2214, 2013.

[17] S. Gopalakannan, S. P. Kumar, V. Premsagar, T. R. Pradeep, "Design, Fabrication and Testing of Regenerative Shock Absorber (Linear Alternator Type)," *International Journal of Applied Engineering Research*, vol. 10, no. 8, pp. 6133-6137, 2015.

[18] B. Scully, L. Zuo, J. Shestani, and Y. Zhou, "Design and characterization of an electromagnetic energy harvester for vehicle suspensions," in *ASME 2009 International Mechanical Engineering Congress and Exposition*, pp. 1007–1016, 2009.

[19] Y. B. Kim, W. G. Hwang, C. D. Kee, H. B. Yi, "Active vibration control of a suspension system using an electromagnetic damper," *Proceedings of the Institution of Mechanical Engineers, Part J Automobile Engineering*, vol. 215, no. 8, pp. 865–873, 2001.

[20] P. Mitcheson and E. Yeatman, "Energy harvesting for pervasive computing," *Perada Magazines*, pp. 1–3, 2008.

[21] P. Múčka, "Energy-harvesting potential of automobile suspension," *Vehicle System Dynamics*, vol. 54, no. 12, pp. 1651–1670, 2016.

[22] M. A. Abdelkareem *et al.*, "Vibration energy harvesting in automotive suspension system: A detailed review," *Appl. Energy*, vol. 229, pp. 672–699, 2018.

[23] R. Zhang, X. Wang, S. John, "A comprehensive review of the techniques on regenerative shock absorber systems," *Energies*, vol. 11, no. 5, pp. 1-67, 2018.

[24] J. Eriksson and S. Piroti, "Review of Methods for Energy Harvesting from a Vehicle Suspension System," Report, KTH Royal Institute of Technology, Sweden, 2016.

[25] Z. Jin-qiu, P. Zhi-zhao, Z. Lei, Z. Yu, "A review on energy-regenerative suspension systems for vehicles," in *Proceedings of the world congress on engineering*, vol. 3, pp. 3–5, 2013.

[26] N. H. Amer, R. Ramli, H. M. Isa, W. N. L. Mahadi, M. A. Z. Abidin, "A review of energy regeneration capabilities in controllable suspension for passengers' car," *Energy Education Science and Technology: Energy Science and Research.*, vol. 30, no. 1, pp. 143–158, 2012.

[27] H. Xiao and X. Wang, "A review of piezoelectric vibration energy harvesting techniques," *Fuel Cells Methanol*, vol. 280, pp. 609-620, 2014.

[28] S. J. Roundy, "Energy scavenging for wireless sensor nodes with a focus on vibration to electricity conversion," PhD Thesis, University of California, Berkeley Berkeley, CA, 2003.

[29] E. Worthington, "Piezoelectric energy harvesting: Enhancing power output by device optimisation and circuit techniques," PhD Thesis, Cranfield University, England, 2010.

[30] S. Priya, "Advances in energy harvesting using low profile piezoelectric transducers," *Journal of Electroceramics*, vol. 19, no. 1, pp. 167–184, 2007.

[31] C. Wei and H. Taghavifar, "A novel approach to energy harvesting from vehicle suspension system: Half-vehicle model," *Energy*, vol. 134, pp. 279–288, 2017.

[32] R. Ambrosio, A. Jimenez, J. Mireles, M. Moreno, K. Monfil, H. Heredia, "Study of piezoelectric energy harvesting system based on PZT," *Integrated Ferroelectrics*, vol. 126, no. 1, pp. 77–86, 2011.

[33] N. Makki and R. Pop-Iliev, "Piezoelectric power generation in automotive tires," *Proc. Smart Mater. Struct. AerospaceNDT Can.*, 2011.

[34] D. J. Leo, *Engineering analysis of smart material systems*. John Wiley & Sons, 2007.

[35] E. Lefeuvre, A. Badel, C. Richard, L. Petit, and D. Guyomar, "A comparison between several vibration-powered piezoelectric generators for standalone systems," *Sensors and Actuators A: Physical.*, vol. 126, no. 2, pp. 405–416, 2006.

[36] PiezoDrive, "PiezoDrive 200V Stack Actuators," Manual and Specifications, University Drive, Australia, pp. 1-3, 2011.

[37] X. Jiang, Y. Li, J. Li, J. Wang, J. Yao, "Piezoelectric energy harvesting from traffic-induced pavement vibrations," *Journal of Renewable and Sustainable Energy*, vol. 6, no. 4, pp. 1-16, 2014.

[38] Y. K. Ramadass and A. P. Chandrakasan, "An efficient piezoelectric energy harvesting interface circuit using a bias-flip rectifier and shared inductor," *IEEE J. Solid-State Circuits*, vol. 45, no. 1, pp. 189–204, 2010.

[39] T. J. Kazmierski and S. Beeby, *Energy harvesting systems*. Springer, 2014.

[40] H. Xiao, X. Wang, S. John, "A dimensionless analysis of a 2DOF piezoelectric vibration energy harvester," *Mechanical Systems and Signal Processing*, vol. 58, pp. 355–375, 2015.

[41] A. Agharkakli, G. S. Sabet, A. Barouz, "Simulation and analysis of passive and active suspension system using quarter car model for different road profile," *International Journal of Engineering Trends and Technology*, vol. 3, no. 5, pp. 636–644, 2012.

[42] C.-Y. Lin, "Material characterization and modeling for piezoelectric actuation and power generation under high electromechanical driving levels," PhD Thesis, Massachusetts Institute of Technology, 2002.

[43] M. Z. Hossain and M. N. A. Chowdhury, "Ride Comfort of a 4 DOF NonLinear Heavy VehicleSuspension," *ISESCO Journal of Science and Technology*, vol. 8, pp. 80–85, 2012.

[44] C. W. De Silva, F. Khoshnoud, M. Li, and S. K. Halgamuge, *Mechatronics: Fundamentals and Applications*. CRC Press, 2015.

[45] ISO 13473-1, "Characterization of pavement texture by use of surface profiles–Part 1: Determination of mean profile depth," *Eur Stand ICS 1714030 Eur Comm Stand Bruss*, pp. 1-47, 1997.

[46] K. Ahlin and N. J. Granlund, "Relating road roughness and vehicle speeds to human whole body vibration and exposure limits," *Int. J. Pavement Eng.*, vol. 3, no. 4, pp. 207–216, 2002.

[47] F. Tyan, Y.-F. Hong, S.-H. Tu, W. S. Jeng, "Generation of random road profiles," *J. Adv. Eng.*, vol. 4, no. 2, pp. 1373–1378, 2009.

[48] S. S. Patole and S. H. Sawant, "Theoretical and numerical analysis of half car vehicle dynamic model subjected to different road profiles with wheel base delay and nonlinear parameters," *International Journal of Multidisciplinary and Current Research*, vol. 3, pp. 542–546, 2015.

[49] D. Al-Yafeai, T. Darabseh, and A-H. I. Mourad, "A State-Of-The-Art Review of Car Suspension-Based Piezoelectric Energy Harvesting Systems," *Energies*, vol. 13, no. 9, pp. 1-39, 2020.

[50] Z. Zhao *et al.*, "Analysis and application of the piezoelectric energy harvester on light electric logistics vehicle suspension systems," *Energy Science & Engineering*, pp. 2741-2755, 2019.

[51] K. Anil and N. Sreeka, "Piezoelectric power generation in tires." *International Journal of Electrical, Electronics and Computer Systems (IJEECS)*, vol. 2, no. 2, 2014

[52] P. Piyush and A. Pandey, "Use of Vibration Energy For Charging Electric Car," *International Journal of Mechanical Engineering & Technology*, vol. 7, no. 2, pp. 59–65, 2016.